The University of Texas at Austin
Chandra Department of Electrical and Computer Engineering
Cockrell School of Engineering

IEEE Forced Oscillation TF, Dec. 2024

Locating the Source of Oscillation with Two-Tier Dynamic Mode Decomposition Integrating Early-Stage Energy

Min-Seung Ko

Postdoctoral Fellow supervised by Dr. Hao Zhu,
Chandra Department of ECE, The University of Texas at Austin

Coauthor: Dr. Wooyoung Shin, Dr. Kai Sun
Advisor: Dr. Kyeon Hur

Contact: kms4634500@utexas.edu

Overview

- Pre- and Post-Mortem Oscillation Framework
  - Pre-Mortem Oscillation Framework
    - How to prevent oscillation which may arise in various frequencies
    - Representative example is impedance-based oscillation analysis
    - Several actions such as adjustment of control gain, can be taken
  - Post-Mortem Oscillation Framework
    - Prior action is to find out the accurate oscillation source as soon as possible
    - Research objective: Generalizable OSL method for both forced and natural cases and both LFO and SSO cases using DMD
    - For more details, please refer to:
      M. -S. Ko, W. Shin, K. Sun and K. Hur, "Locating the Source of Oscillation With Two-Tier Dynamic Mode Decomposition Integrating Early-Stage Energy," in IEEE Transactions on Power Systems, vol. 39, no. 4, pp. 5535-5547, July 2024

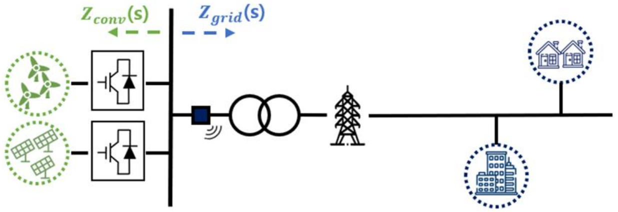

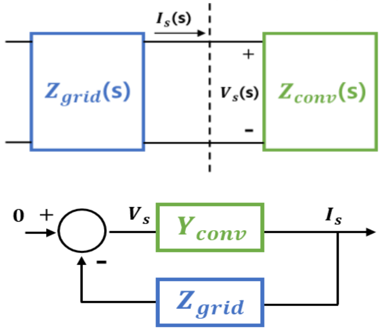

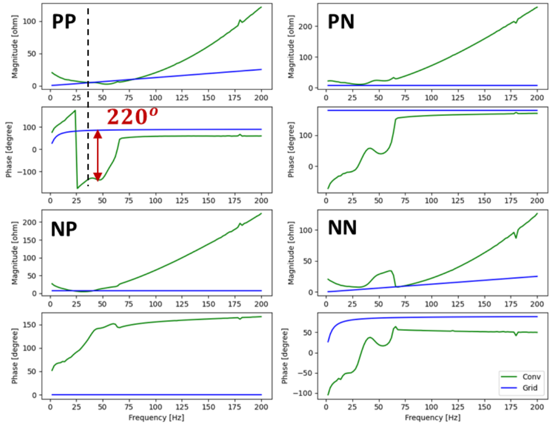

$$\Delta i_s = \frac{Y_{conv}(s)}{1 + Y_{conv}(s) Z_{grid}(s)} \Delta v_s$$

<Example of impedance-based analysis>

IEEE TRANSACTIONS ON POWER SYSTEMS, VOL. 39, NO. 4, JULY 2024 5535

Locating the Source of Oscillation With Two-Tier Dynamic Mode Decomposition Integrating Early-Stage Energy

Min-Seung Ko, *Graduate Student Member, IEEE*, Wooyoung Shin, *Member, IEEE*, Kai Sun, *Senior Member, IEEE*, and Kyeon Hur, *Senior Member, IEEE*

Preliminaries

- Mathematical formulation of Singular Value Decomposition (SVD)
  - Generalized eigen-decomposition of a square matrix into two unitary matrices and one diagonal matrix
  - SVD can be regarded as the data dimensionality reduction method, since key features of the correlation matrix can be drawn from large data

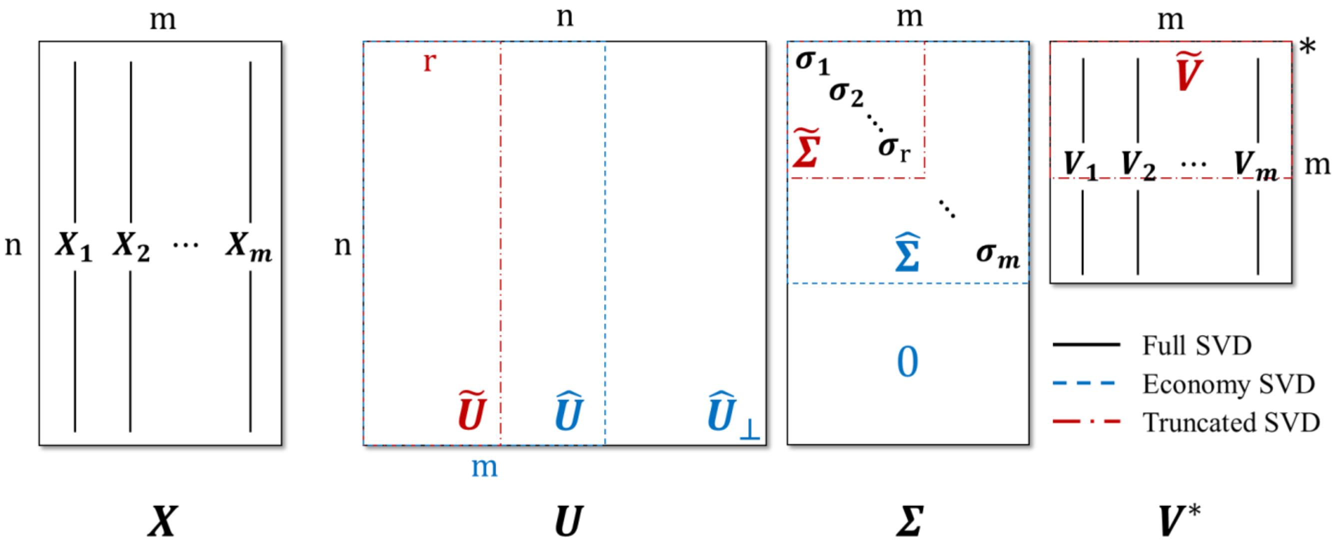

<Schematic diagram of SVD>

$$\begin{aligned} \boldsymbol{X} &= \boldsymbol{U\Sigma V}^* \text{ : Full SVD} \\ &= \hat{\boldsymbol{U}}\hat{\boldsymbol{\Sigma}}\boldsymbol{V}^* \text{ : Economy SVD} \\ &\approx \tilde{\boldsymbol{U}}\tilde{\boldsymbol{\Sigma}}\tilde{\boldsymbol{V}}^* \text{ : Truncated SVD} \end{aligned}$$

where $\boldsymbol{U} = [\boldsymbol{u}_1\boldsymbol{u}_2 \cdots \boldsymbol{u}_n]$, $\boldsymbol{V} = [\boldsymbol{v}_1\boldsymbol{v}_2 \cdots \boldsymbol{v}_m]$,
$\boldsymbol{\Sigma} = [\hat{\boldsymbol{\Sigma}}\ \boldsymbol{0}]^T$, $\hat{\boldsymbol{\Sigma}} = \text{diag}(\sigma_1, \sigma_2, \cdots, \sigma_m)$

Eigen-decomposition feature:

$$\boldsymbol{X}^T\boldsymbol{X} = \left(\hat{\boldsymbol{U}}\hat{\boldsymbol{\Sigma}}\boldsymbol{V}^T\right)^T\left(\hat{\boldsymbol{U}}\hat{\boldsymbol{\Sigma}}\boldsymbol{V}^T\right) = \boldsymbol{V}\hat{\boldsymbol{\Sigma}}^2\boldsymbol{V}^T$$

$$\Rightarrow \boldsymbol{X}^T\boldsymbol{X}\boldsymbol{V} = \boldsymbol{V}\hat{\boldsymbol{\Sigma}}^2$$

Preliminaries

* S. L. Brunton and J. N. Kutz, Data-Driven Science and Engineering: Machine Learning, Dynamical Systems, and Control. Cambridge, U.K.: Cambridge Univ. Press, 2019.

- Derivation of Dynamic Mode Decomposition (DMD) as a spatiotemporal SVD*
  - Eckart-Young's Theorem
    - For the linearized objective system $\boldsymbol{X}' = \boldsymbol{A}\boldsymbol{X}$, the best rank-$r$ approximation of $\boldsymbol{X}$ can be drawn from rank-r truncated SVD of $\boldsymbol{X}$ as:

$$\text{argmin}_{\tilde{\boldsymbol{X}}} ||\boldsymbol{X} - \tilde{\boldsymbol{X}}|| \approx \tilde{\boldsymbol{U}}\tilde{\boldsymbol{\Sigma}}\tilde{\boldsymbol{V}}^* \text{ s.t. } \text{rank}(\tilde{\boldsymbol{X}}) = r$$

$\boldsymbol{X}$: present measurement matrix
$\boldsymbol{X}'$: future measurement matrix
$\boldsymbol{A}$: best-fit linear operator

  - Derivation of DMD
    - If we substitute the truncated SVD into the objective system, we can get

$$\boldsymbol{X}' = \boldsymbol{A}\boldsymbol{X} \approx \boldsymbol{A}\tilde{\boldsymbol{U}}\tilde{\boldsymbol{\Sigma}}\tilde{\boldsymbol{V}}^* \rightarrow \boldsymbol{A} = \boldsymbol{X}'\tilde{\boldsymbol{V}}\tilde{\boldsymbol{\Sigma}}^{-1}\tilde{\boldsymbol{U}}^*$$

    - Then, $\tilde{\boldsymbol{A}}$, which is the projection of $\boldsymbol{A}$ onto $\tilde{\boldsymbol{U}}$, can be calculated as

$$\tilde{\boldsymbol{A}} = \tilde{\boldsymbol{U}}^*\boldsymbol{A}\tilde{\boldsymbol{U}} = \tilde{\boldsymbol{U}}^*\boldsymbol{X}'\tilde{\boldsymbol{V}}\tilde{\boldsymbol{\Sigma}}^{-1}$$

    - If we let $\boldsymbol{\Lambda}$ and $\boldsymbol{W}$ as the eigenvalues and eigenvectors of $\tilde{\boldsymbol{A}}$, i.e., $\tilde{\boldsymbol{A}}\boldsymbol{W} = \boldsymbol{W}\boldsymbol{\Lambda}$, $\boldsymbol{X}'$ can be modified as

$$\boldsymbol{X}' = \tilde{\boldsymbol{U}}\boldsymbol{W}\boldsymbol{\Lambda}\boldsymbol{W}^{-1}\tilde{\boldsymbol{\Sigma}}\tilde{\boldsymbol{V}}^* = \boldsymbol{\Phi}\boldsymbol{\Lambda}\boldsymbol{\Gamma}$$

$\boldsymbol{\Phi} = \tilde{\boldsymbol{U}}\boldsymbol{W}$: DMD mode
$\boldsymbol{\Gamma} = \boldsymbol{W}^{-1}\tilde{\boldsymbol{\Sigma}}\tilde{\boldsymbol{V}}^*$: temporal distribution of mode amplitude
$\boldsymbol{\Lambda}$: empirical Ritz values (includes oscillation frequency information)

Preliminaries

- Derivation of Dynamic Mode Decomposition (DMD) as a spatiotemporal SVD*

(1) Objective System :

$$\underbrace{\begin{bmatrix}\Delta V_{2\sim m}\\ \Delta\theta_{2\sim m}\end{bmatrix}}_{X'\ (2l \times (m-1))} = \underbrace{A}_{2l \times 2l} \underbrace{\begin{bmatrix}\Delta V_{1\sim m-1}\\ \Delta\theta_{1\sim m-1}\end{bmatrix}}_{X\ (2l \times (m-1))}$$

(2) SVD:

$$\underbrace{\begin{bmatrix}\Delta V_{1\sim m-1}\\ \Delta\theta_{1\sim m-1}\end{bmatrix}}_{X} = \underbrace{U}_{2l \times 2l}\ \underbrace{\Sigma}_{2l \times 2l}\ \underbrace{V^*}_{2l \times (m-1)}$$

(3) = (1)+(2):

$$A = X' V \Sigma^{-1} U^*$$

(4) Projection:

$$\tilde{A} = U^* A U$$

(5) = (3)+(4):

$$\tilde{A} = U^* X' V \Sigma^{-1}$$

(6) Eigen analysis:

$$\tilde{A} = W \Lambda W^{-1}$$

(7) = (5)+(6):

$$X' = \underbrace{U W}_{\Phi}\ \Lambda\ \underbrace{W^{-1} \Sigma V^*}_{\Gamma}$$

This computation process is a specific case used for OSL

* S. L. Brunton and J. N. Kutz, Data-Driven Science and Engineering: Machine Learning, Dynamical Systems, and Control. Cambridge, U.K.: Cambridge Univ. Press, 2019.

DMD on Power System Oscillation

- Analysis of Power System Oscillation with DMD**

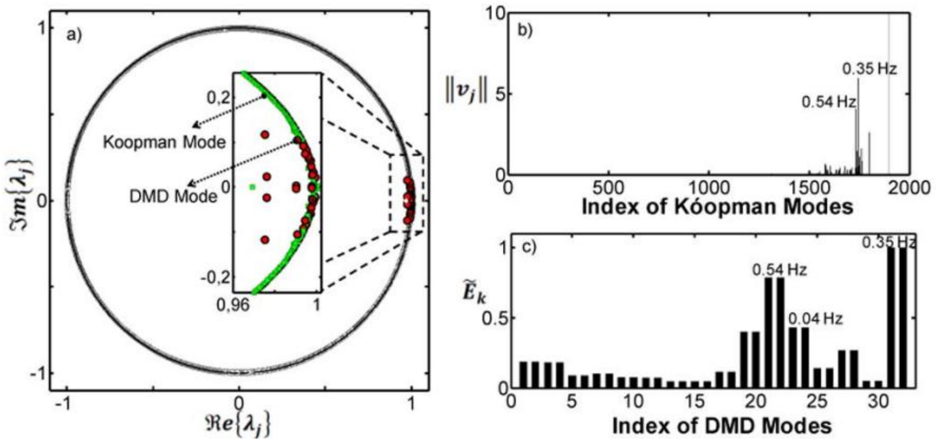

<Estimated empirical Ritz value>

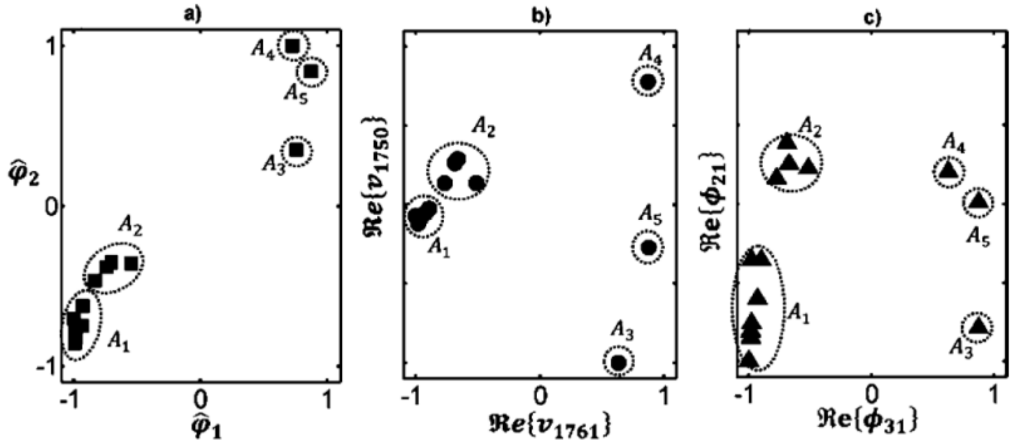

<Coherency identification with (a) POD, (b) Koopman, and (c) DMD>

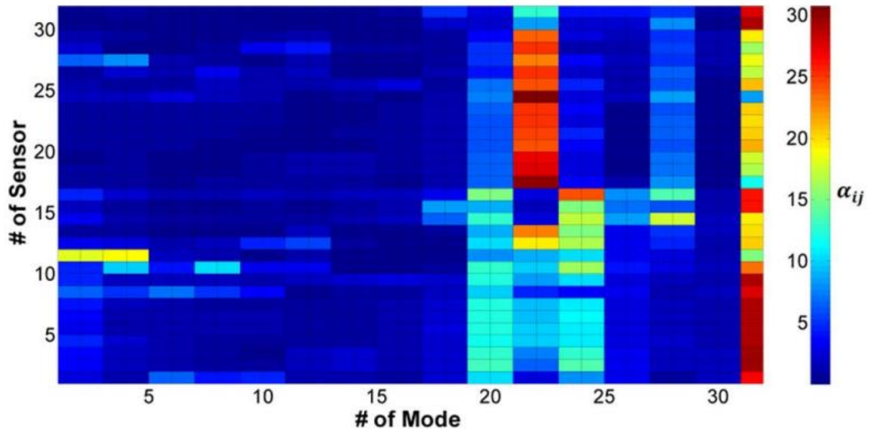

<Dominant mode analysis>

** E. Barocio, et al., “A dynamic mode decomposition framework for global power system oscillation analysis,” IEEE Trans. Power Syst., vol. 30, no. 6, pp. 2902–2912, Nov. 2015.

DMD on Power System Oscillation

- Limitations of DMD on Oscillation Source Location (OSL)
  - No previous research to apply DMD for oscillation source location
    - Framework and details of DMD are not specified for OSL
  - DMD cannot be ensured to be effective for abnormal oscillation cases
    - (Category 2) Maximum oscillation is observed at non-source bus
    - (Category 3) Rectangular forcing signal injected
    - (Category 4) Measurements at the source bus do not exits
    - (Category 5) Other abnormal cases

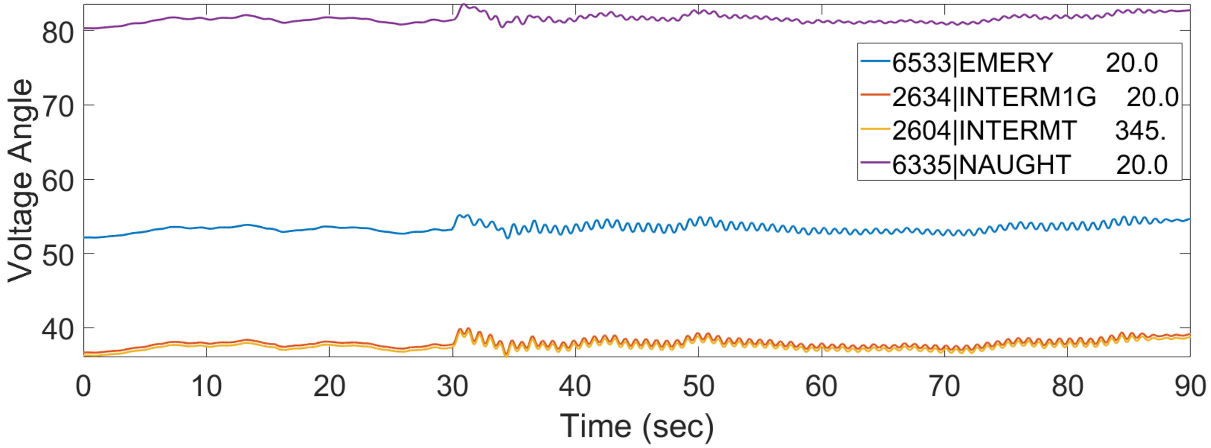

<Voltage angle of NASPI case #2>

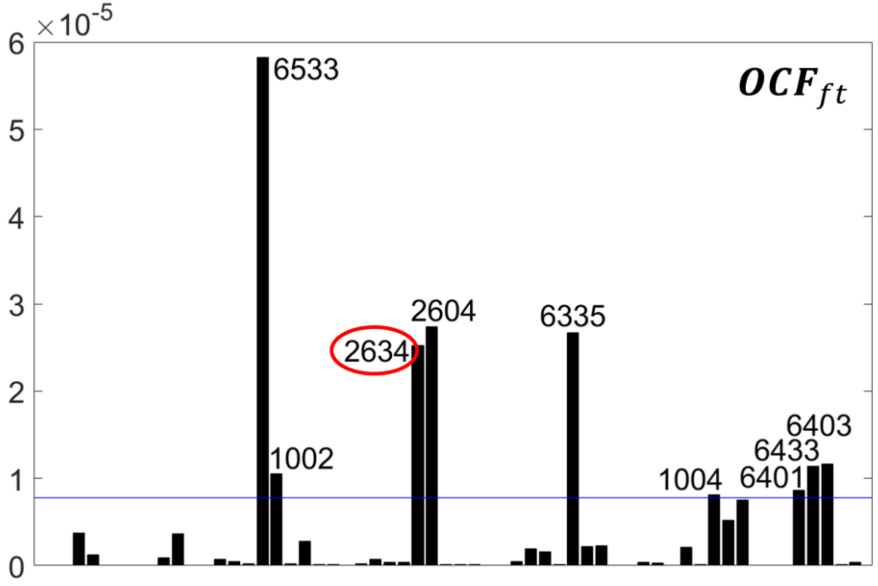

<Mode magnitude analysis of NASPI case #2>

Contributions of the Proposed Method

- Extend the usage of DMD into oscillation source location
- Construct the oscillation monitoring framework via DMD
- Formulate the **improved DMD**

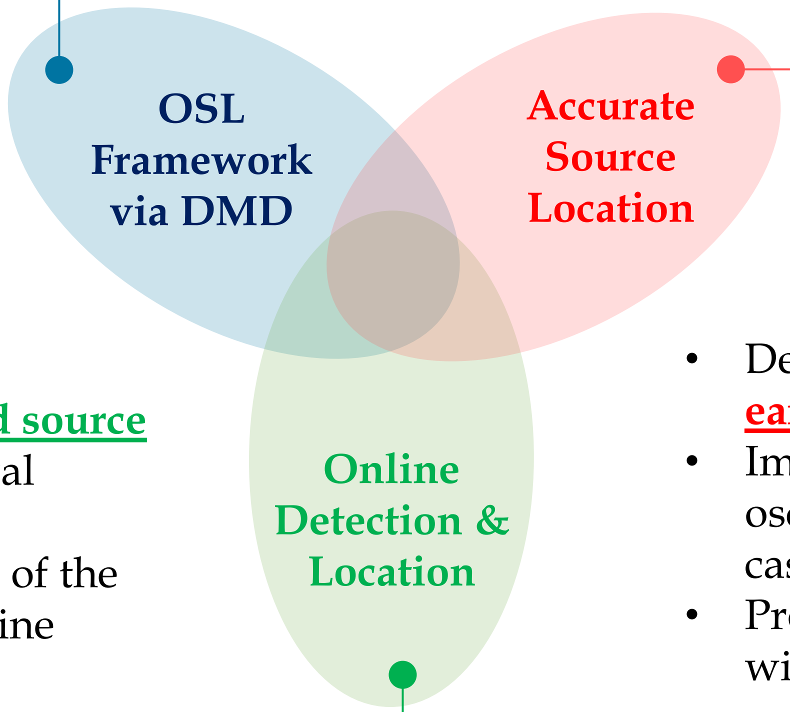

- Develop the **oscillation detection and source location method** using spatio-temporal analysis results from DMD
- Enhance the computational efficiency of the oscillation monitoring scheme for online application

- Develop the **two-tier structure to identify the early-stage oscillatory energy**
- Improve the location accuracy across various oscillation scenarios for both forced and natural cases
- Provide data preprocessing method to deal with the real oscillation case

Improved DMD

- Modifying DMDc into improved DMD

*** J. L. Proctor, S. L. Brunton, and J. N. Kutz, "Dynamic mode decomposition with control," SIAM Journal on Applied Dynamical Systems 15.1 (2016): 142-161.

  - DMDc*** (DMD with control) inserts current control signals as an additional input to divide the control from the system dynamics
  - Improved DMD for oscillation monitoring replaces the control signal with the initial state of the measurement matrix

$$\boldsymbol{X}' = \boldsymbol{A}\boldsymbol{X} + \boxed{\boldsymbol{B}\boldsymbol{X}_{ini}} = [\boldsymbol{A}\ \ \boldsymbol{B}][\boldsymbol{X}\ \ \boldsymbol{X}_{ini}]^T = \boldsymbol{G}\boldsymbol{\Omega}$$

$\boldsymbol{X}_{ini}$: initial state of the measurement matrix

Assume that $f(k)$ denotes a function describing the oscillation dynamics for every discrete time of the measurements, $k \in (1,2,\dots,m-1)$, the future matrix can be represented as

$$\boldsymbol{X}_{k+1} = \boldsymbol{A}\boldsymbol{X}_k + \boldsymbol{B}\boldsymbol{X}_{ini} = \boldsymbol{X}_{ini} + f(k)$$

$$\Longrightarrow \boldsymbol{X}_2 = \boldsymbol{A}\boldsymbol{X}_{ini} + \boldsymbol{B}\boldsymbol{X}_{ini} = \boldsymbol{X}_{ini} + f(1)$$
$$\Longrightarrow \boldsymbol{B}\boldsymbol{X}_{ini} = (\boldsymbol{I} - \boldsymbol{A})\boldsymbol{X}_{ini} + f(1)$$
$$\Longrightarrow \boxed{\boldsymbol{A}(\boldsymbol{X}_k - \boldsymbol{X}_{ini}) = f(k) - f(1)}$$

∴ The state matrix $\boldsymbol{A}$ represents the linear relationship between the change of the states and change of the oscillation dynamics ($\boldsymbol{A}$ can focus on the post-mortem modified dynamics, $\boldsymbol{B}$ takes the basic dynamics driven by the initial state)

Improved DMD

- Improved DMD Computation

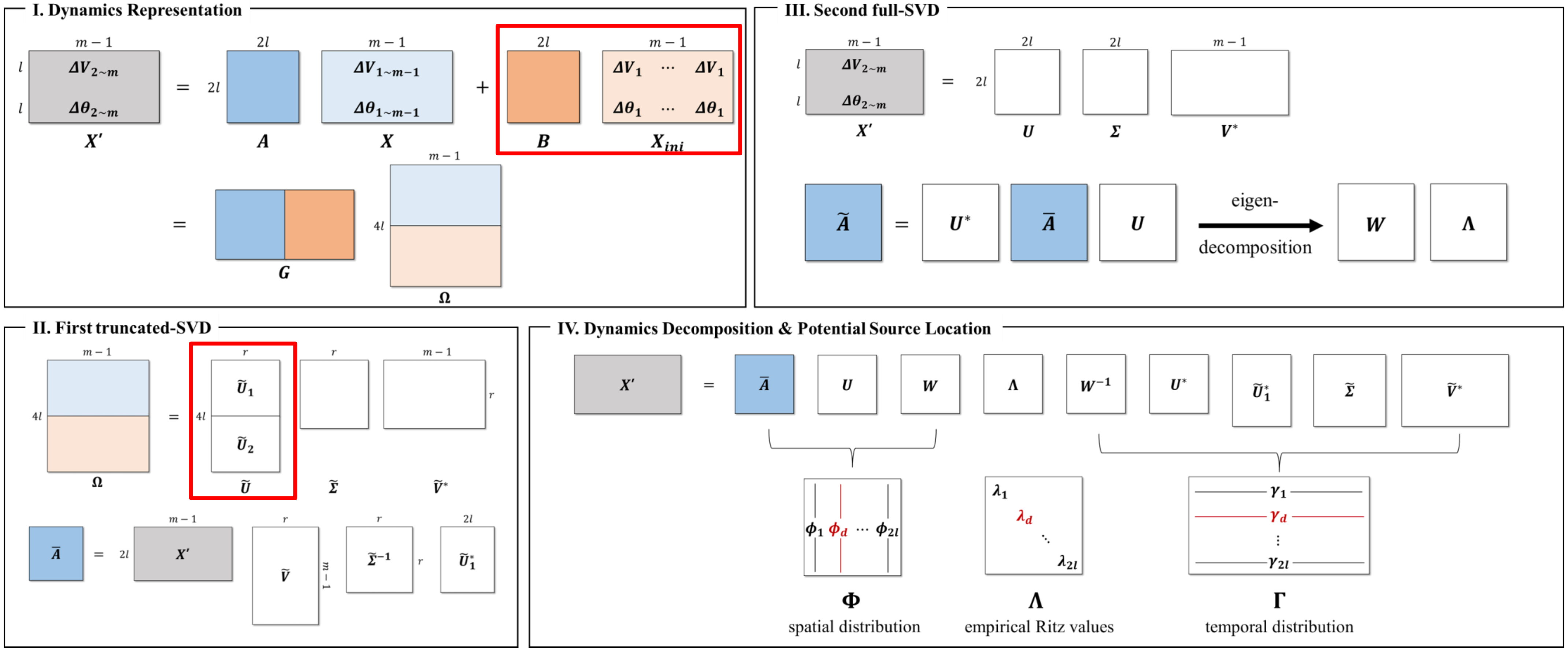

Proposed Framework

- Framework Overview

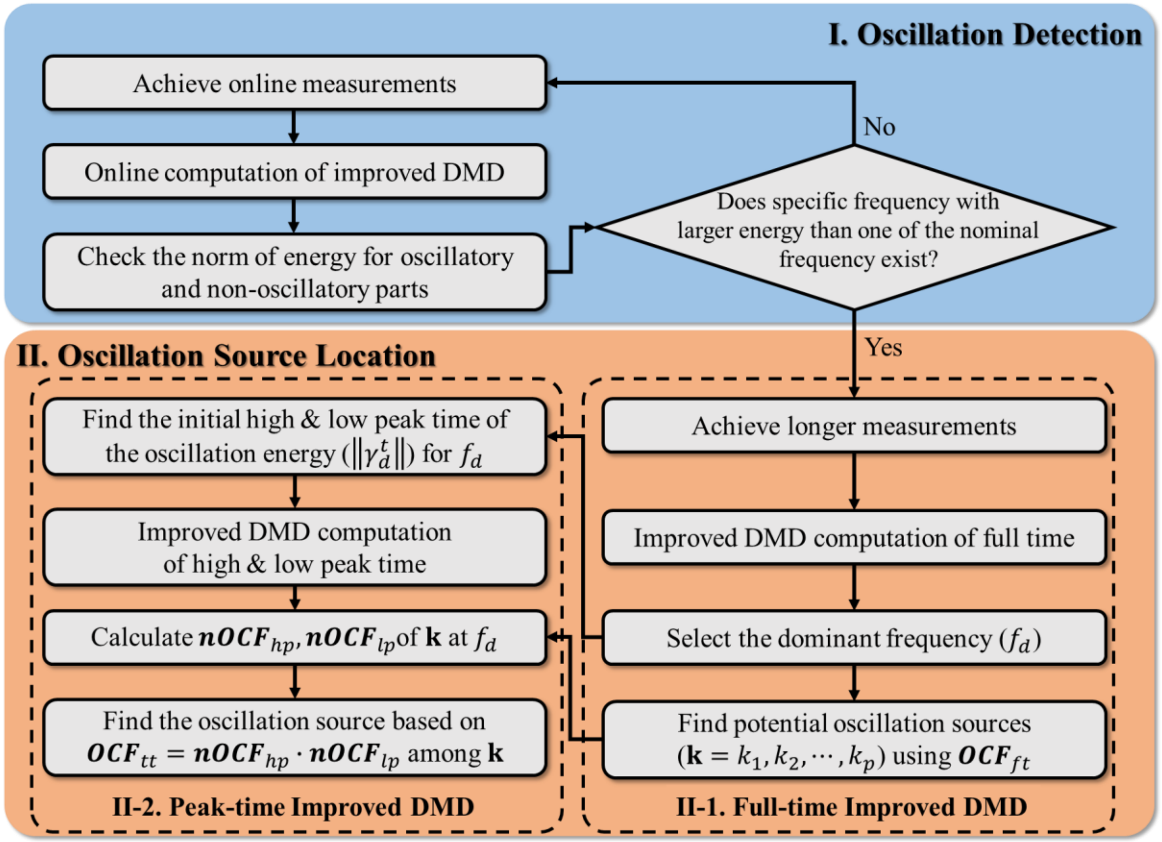

<Oscillation detection & source location framework>

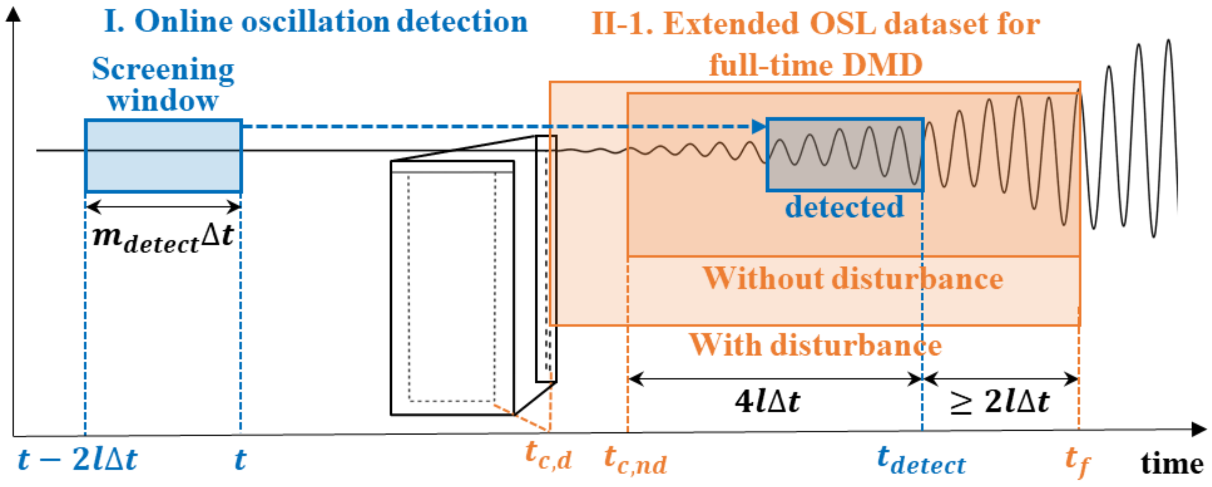

<Timeline of detection and source location>

Proposed Framework

- Online Oscillation Detection
  - Size of detection screening window
    - Length of the measurement matrix should be larger than rank r for the truncated SVD: $m_{detect} \geq r = 2l$
    - The size needs to be as short as possible to guarantee online detection : $m_{detect} = 2l$
  - Oscillation detection
    - $\Lambda|_t$ and $\Gamma|_t$ can be achieved by the DMD computation for the measurement from $t - m_{detect}\Delta t$ to t
    - Oscillation exists if the following condition is not met:

$$\forall i \in (1,2,\ldots,2l) \text{ and } i \neq i_0, ||\gamma_{i0}|_t|| > \alpha \cdot ||\gamma_i|_t||$$

$$\text{s.t. } f_{i_0}^t = 0, \alpha = 3$$

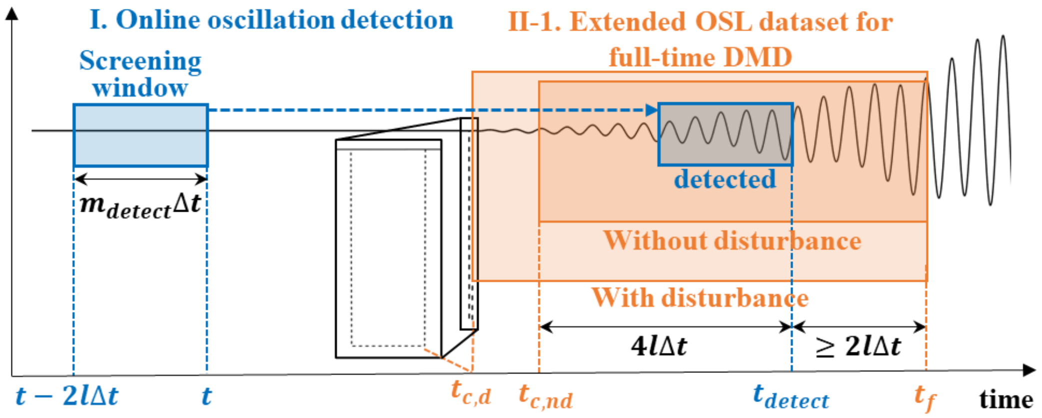

<Timeline of detection and source location>

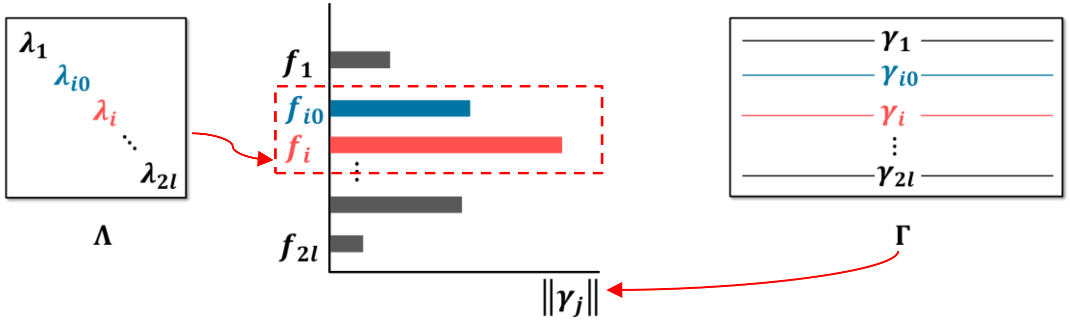

<Oscillation detection process using improved DMD>

Proposed Framework

- Oscillation Source Location
  - Size of location screening window
    - The screening window for OSL is extended for more detailed analysis
    - Minimum condition for t_f: $t_f - t_{detect} \geq 2l\Delta t$
    - Critical time t_c is selected differently according to the existence of the disturbance[1)] in the measurements: With disturbance, $t_{c,d}$ is equal to the fault clearing time. Without disturbance, $t_{c,n} = t_{detect} - 4l\Delta t$

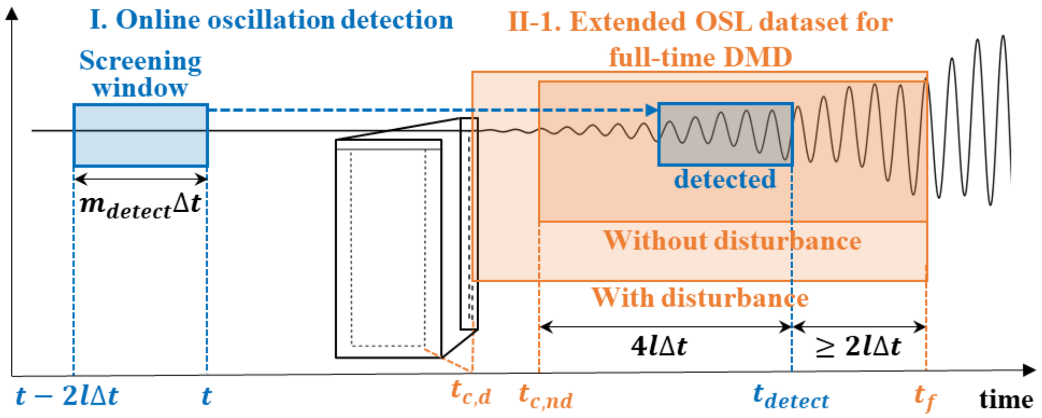

<Timeline of detection and source location>

1) Disturbance types of interest includes momentary sag, swell, and surge by short circuits, major equipment shutdown, etc., which mostly appear as impulse signals.

Proposed Framework

- Oscillation Source Location
  - Proposed source location framework
    - First stage: compute full-time improved DMD, specify potential oscillation sources
    - Second stage: oscillatory energy at the early stage is analyzed to identify the source
  - First stage of OSL
    - With similar process to detection, find out dominant frequency f_d
    - Select potential oscillation sources $\boldsymbol{k} = [k_1, k_2, \dots, k_p]$ based on Oscillation Contribution Factor for full time $(\mathbf{OCF}_{ft})$

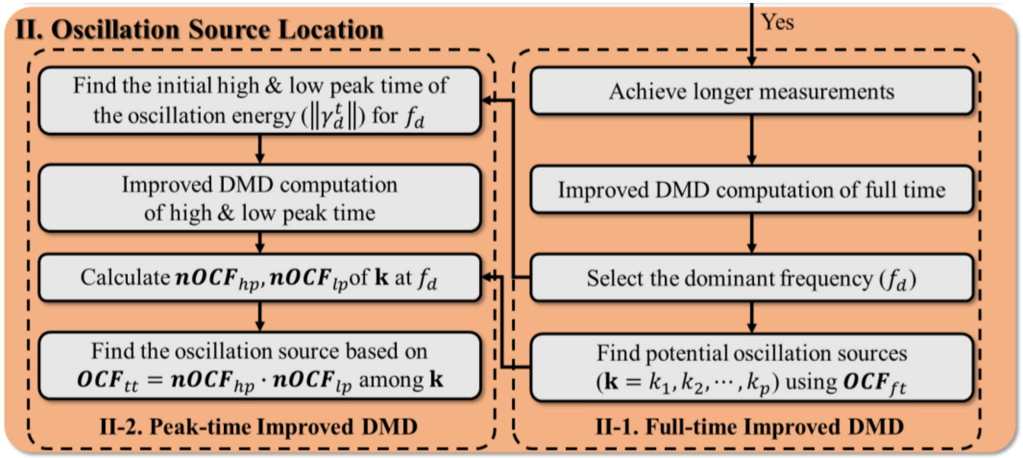

<Process of OSL framework>

$$\mathbf{OCF}_{ft} = |\mathbf{MM}_v^{ft} \cdot \mathbf{MM}_\theta^{ft}|$$

$$\text{s.t.} \quad \mathbf{MM}_v^{ft} = \frac{\mathcal{Re}\{\phi_{d,v}\} \cdot \mathcal{Im}\{\phi_{d,v}\}}{\sqrt{\mathcal{Re}\{\phi_{d,v}\}^2 + \mathcal{Im}\{\phi_{d,v}\}^2}},$$

$$\mathbf{MM}_\theta^{ft} = \frac{\mathcal{Re}\{\phi_{d,\theta}\} \cdot \mathcal{Im}\{\phi_{d,\theta}\}}{\sqrt{\mathcal{Re}\{\phi_{d,\theta}\}^2 + \mathcal{Im}\{\phi_{d,\theta}\}^2}}$$

Proposed Framework

- Oscillation Source Location
  - Second stage of OSL
    - Early-stage oscillatory energy can be calculated by comparing the two peak-time DMD results subtracted by full-time DMD
    - High and low peak times are determined on the first swing of temporal oscillation energy, $||\gamma_d^t|_{t_f}||$
    - The final oscillation contribution factor to identify the oscillation source is given by:

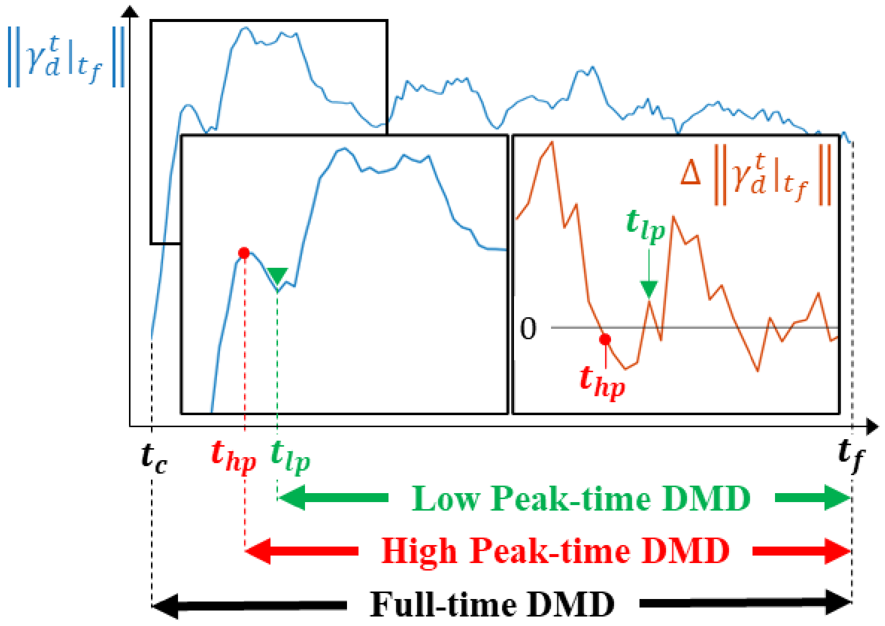

<Graphical representation of peak times>

$$\mathbf{OCF}_{tt} = |\mathbf{nOCF}_{hp} \cdot \mathbf{nOCF}_{lp}|$$

s. t.

$$\mathbf{nOCF}_{hp,lp} = \left[\mathrm{nOCF}_{k_1}^{hp,lp}, \mathrm{nOCF}_{k_2}^{hp,lp}, \dots, \mathrm{nOCF}_{k_p}^{hp,lp}\right],$$

$$\mathrm{nOCF}_{k}^{hp,lp} = \frac{\mathrm{OCF}_{k}^{hp,lp}}{\max(\mathrm{OCF}_{k\in\mathbf{k}}^{hp,lp})},$$

$$\mathbf{OCF}_{hp,lp} = |(\mathbf{MM}_{v}^{ft} - \mathbf{MM}_{v}^{hp,lp}) \cdot (\mathbf{MM}_{\theta}^{ft} - \mathbf{MM}_{\theta}^{hp,lp})|$$

Experimental Results on LFO

- Oscillation dataset
  - Simulated cases (TSAT, WECC 179 bus system)
  - 2021 NASPI contest cases (TSAT, WECC 240 bus system)
  - Real oscillation cases (ISO-NE)
  - Source: https://web.eecs.utk.edu/~kaisun/Oscillation/
- Overall Results

Category	Tested Cases	Oscillation Frequency	Oscillation Source	Estimated Frequency	Estimation Error	Estimated Source	Elapsed Location Time
Category 1	Sim 2F	0.86 Hz	Bus 79	0.8567 Hz	0.38%	Bus 79	0.41s
	Sim 6ND	1.408 Hz	Bus 45, 159	1.402 Hz	0.42%	Bus 45, 159	0.46s
	NASPI 7	0.379 Hz	Bus 2634	0.3751 Hz	1.03%	Bus 2634	0.57s
Category 2	Sim 3F	0.37 Hz	Bus 77	0.3680 Hz	0.54%	Bus 77	0.57s
	Sim 1ND	1.408 Hz	Bus 45	1.3991 Hz	0.63%	Bus 45	0.46s
	NASPI 2	1.19 Hz	Bus 2634	1.1885 Hz	0.12%	Bus 2634	0.52s
	NASPI 8	0.614 Hz	Bus 6333	0.6160 Hz	0.32%	Bus 6333	0.92s
Category 3	Sim 6F3	0.4 Hz	Bus 79	0.4025 Hz	0.63%	Bus 79	0.47s
	NASPI 12	0.37 Hz	Bus 6335	0.3739 Hz	1.05%	Bus 6335	0.63s
Category 4	NASPI 3	0.379 Hz	Bus 1131	0.3788 Hz	0.05%	Bus 1131 or 1032	0.86s
Category 5	NASPI 13	0.614 Hz	Bus 2619	0.6149 Hz	0.15%	Bus 2619	1.02s

(a)

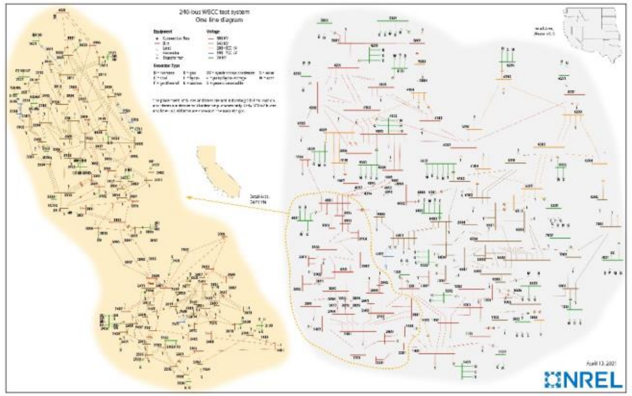

(b)

<One-line diagram of (a) WECC 179 bus system and (b) WECC 240 bus system>

※ Sim: Simulated cases on WECC 179 bus system, NASPI: NASPI cases on WECC 240 bus system, F: Forced oscillation, N: Natural oscillation

Experimental Results on LFO

- OSL for Normal Oscillation Case

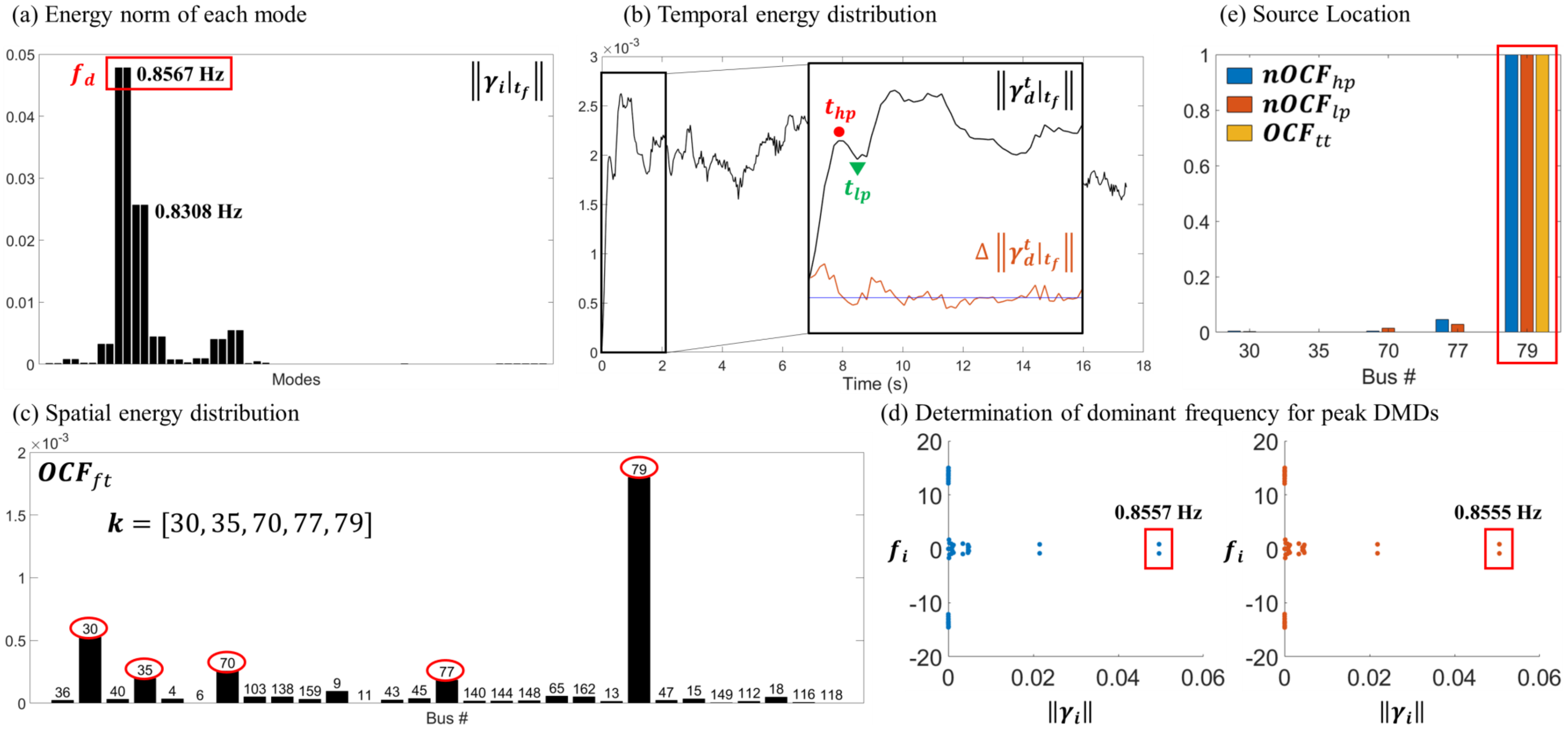

<Oscillation source location process for Sim 2F case>

Experimental Results on LFO

- OSL for Maximum Oscillation on Non-Source Bus

NASPI 2

NASPI 8

(a) Choice of peak times

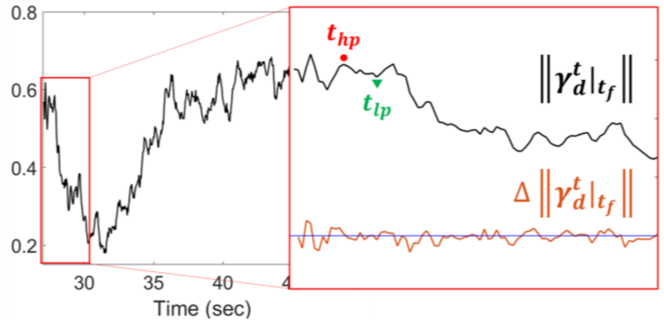

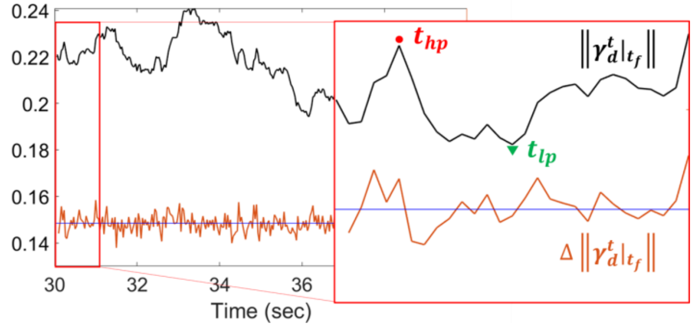

(b) OCF_{ft}

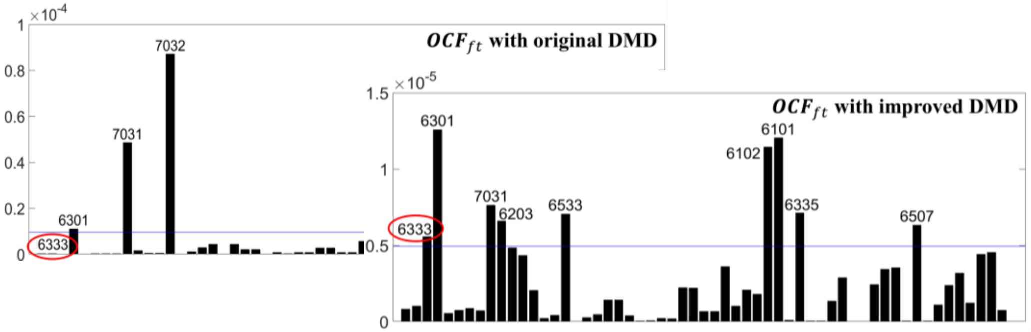

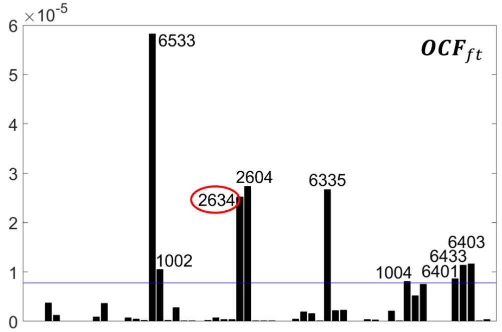

(c) OCF_{tt}

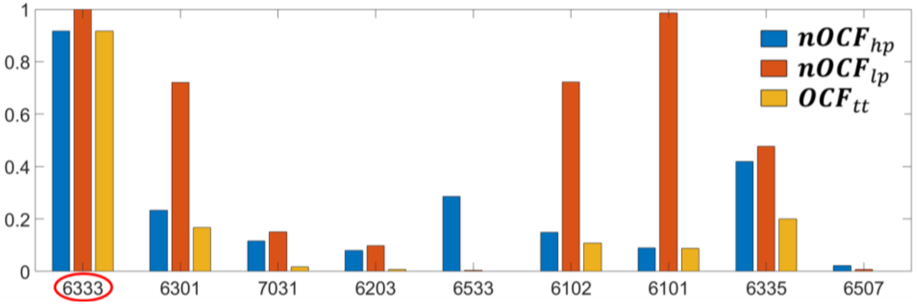

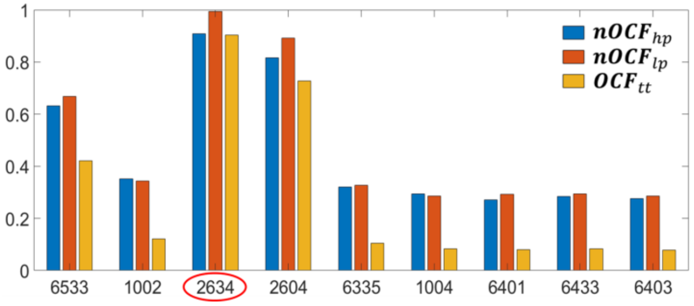

Experimental Results on LFO

- OSL for Rectangular Signal Injection & Unmonitored Cases

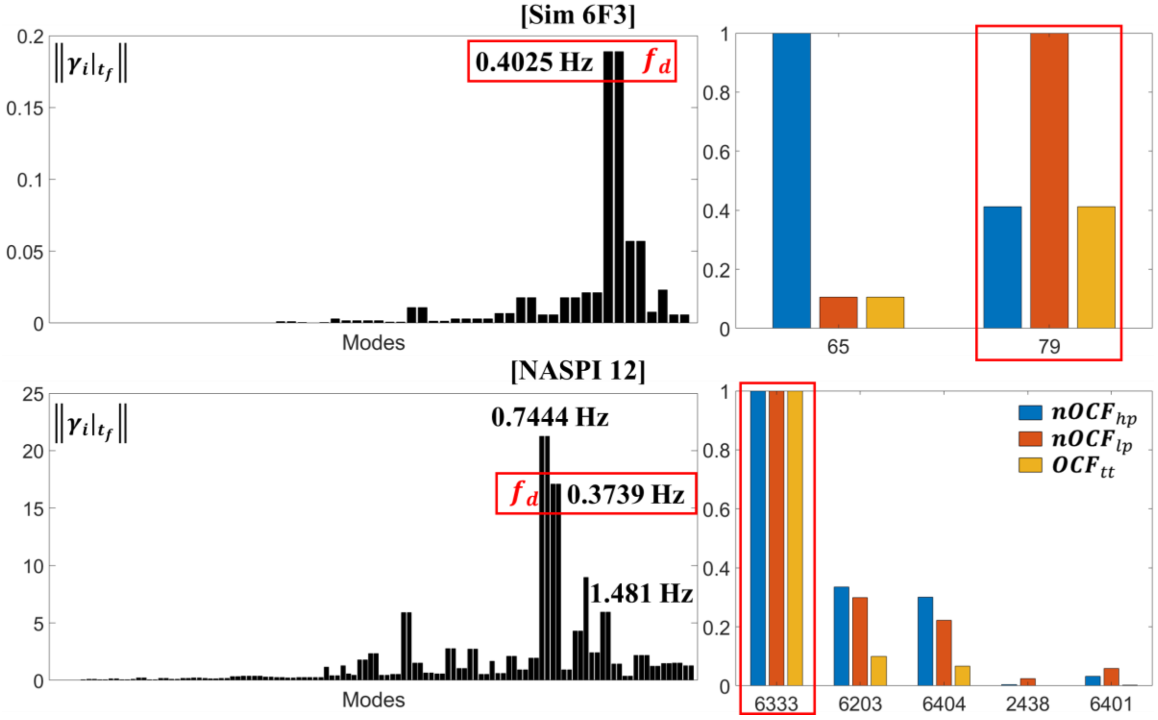

<Schematic diagram of the simulation results for the third category cases>

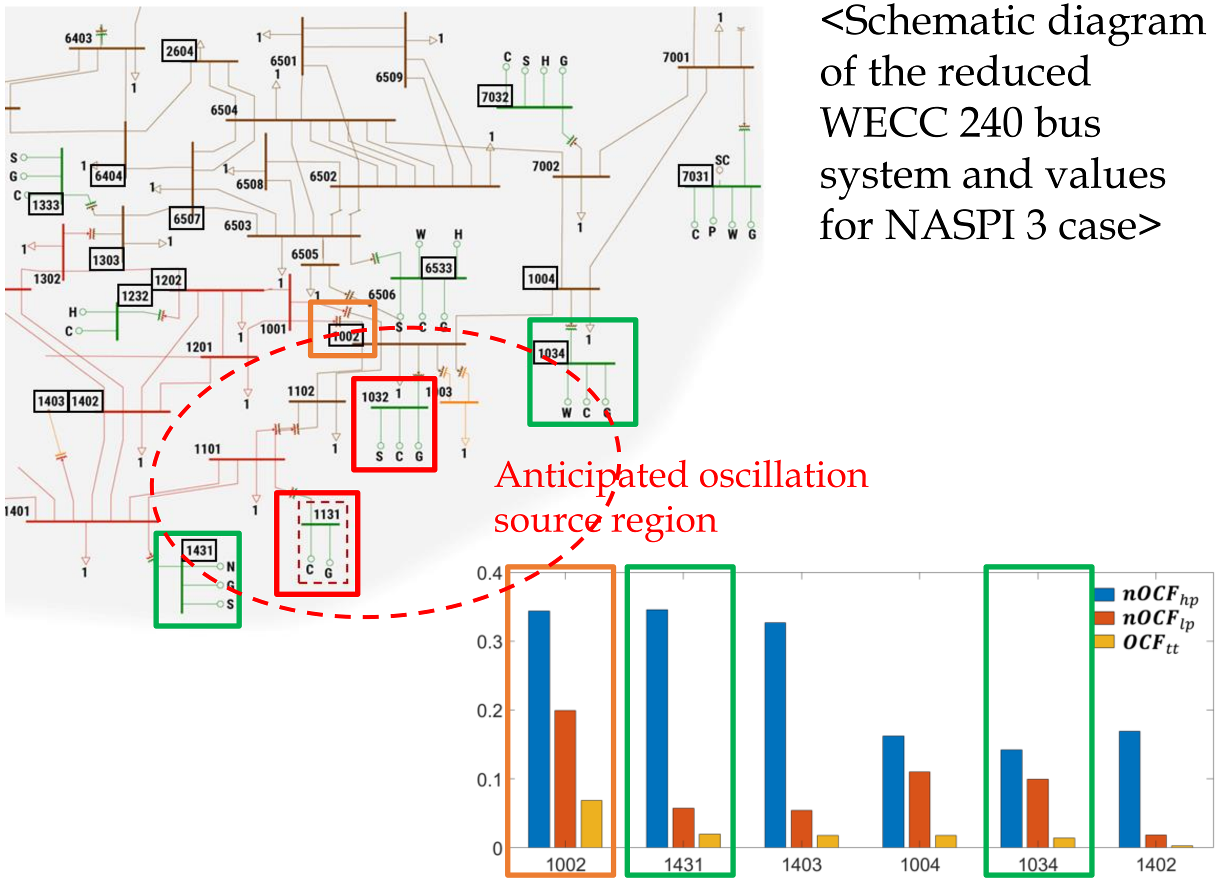

<Schematic diagram of the reduced WECC 240 bus system and values for NASPI 3 case>

Experimental Results on LFO

- OSL for Real Oscillation Case

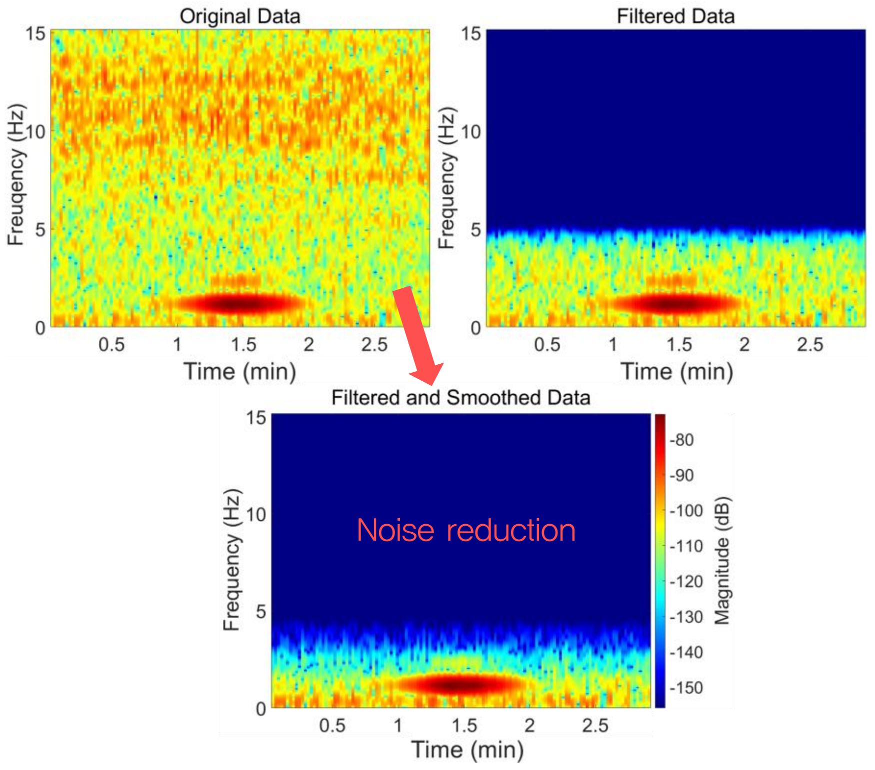

<Power spectra for original, filtered, and filtered & smoothed data>

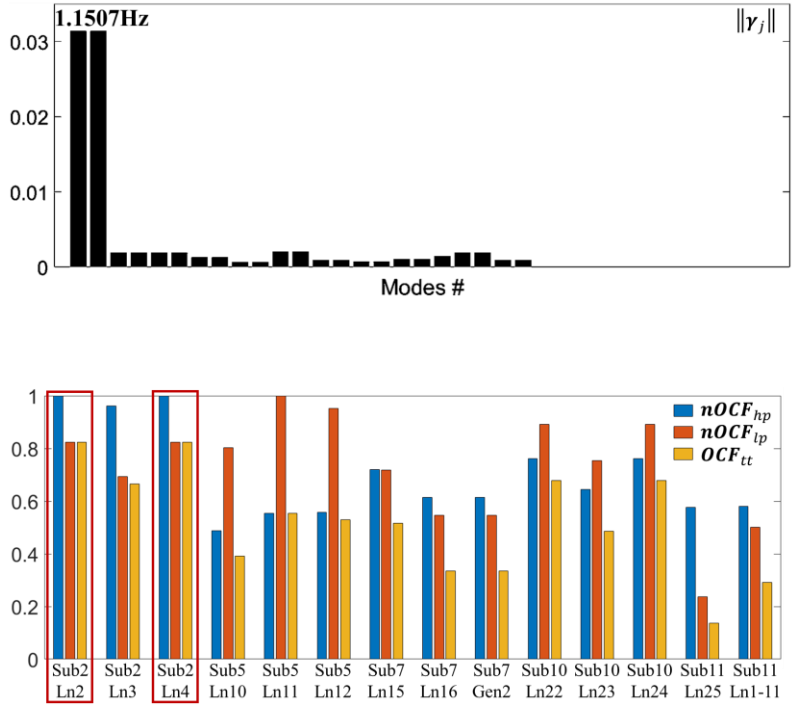

<Schematic diagrams of the dominant frequency and OCF_{tt} values>

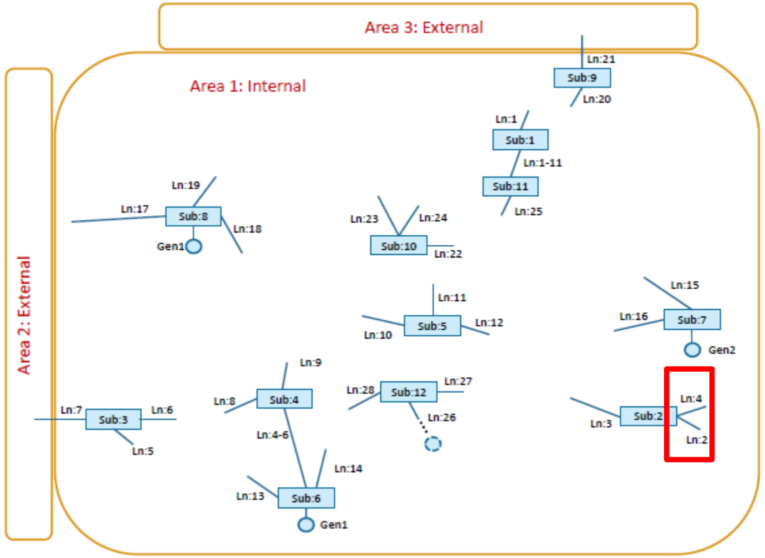

<ISO-NE map>

Experimental Results on SSO

- Oscillation dataset
  - Simulated cases (PSCAD, IEEE 39 bus system)
    - Case 1: 23 Hz forcing signal injection in Bus 38
    - Case 2: 23 Hz forcing signal injection in Bus 39
    - Assume only line voltage magnitude & phase angle measurements

Case 1

Case 2

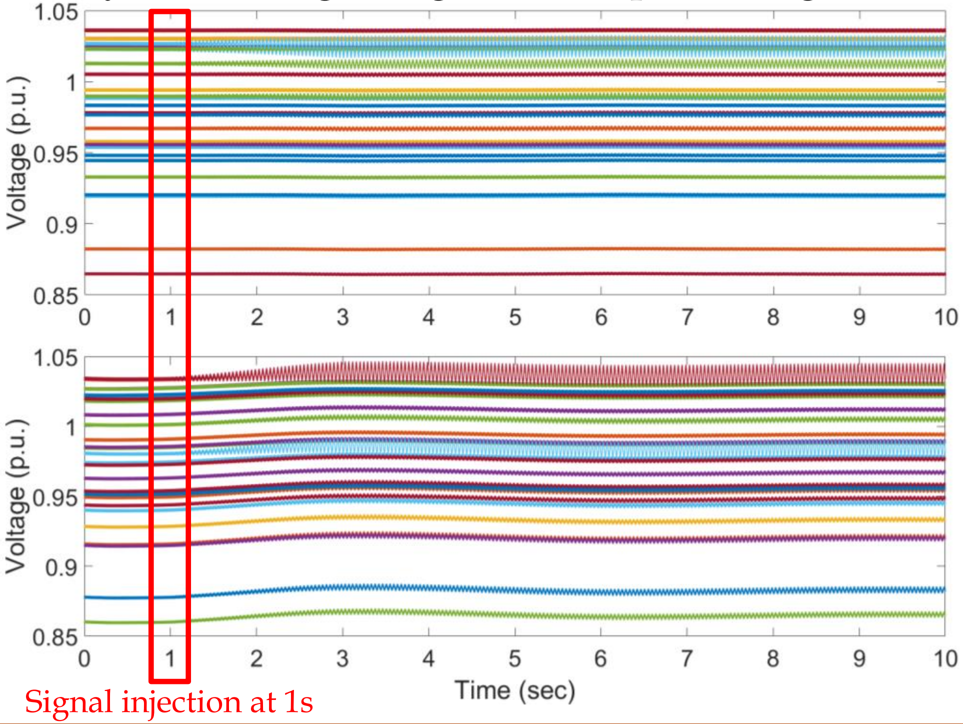

Signal injection at 1s

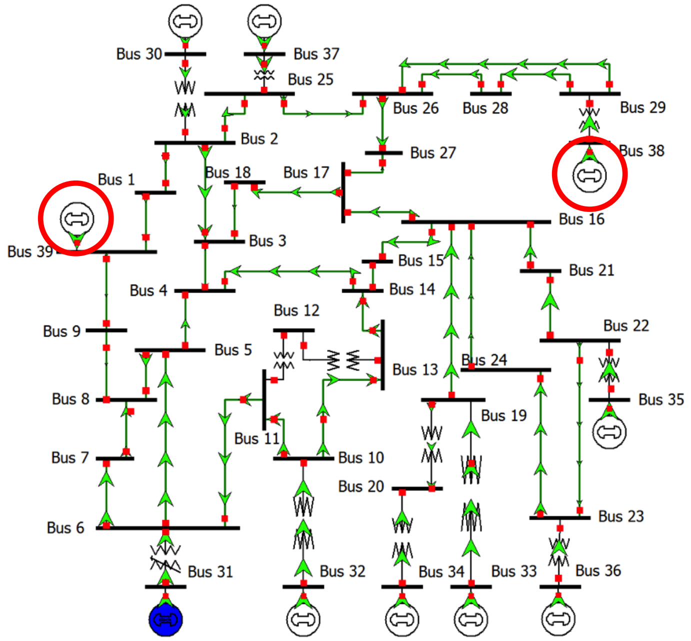

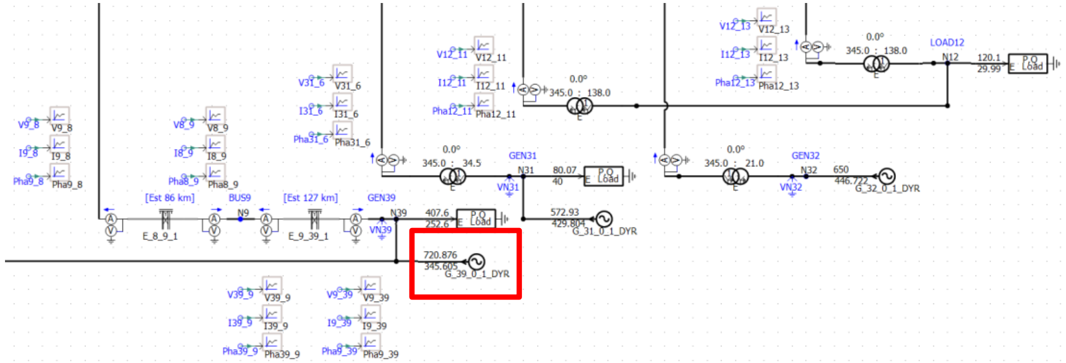

Experimental Results on SSO

- Differences from LFO Case
  - Problem
    - Difference with LFO in interested frequency and measuring frequency ($F_s = 10000$ Hz)
    - Ripples observed in all time span
  - Strategy
    - Preprocessing is required for simulation data: 60 Hz LPF & Smoothing
    - Extension of window size: $m_{detect} = 2l \rightarrow 20l$ (1.5s for detection, 3s for OSL in SSO case)

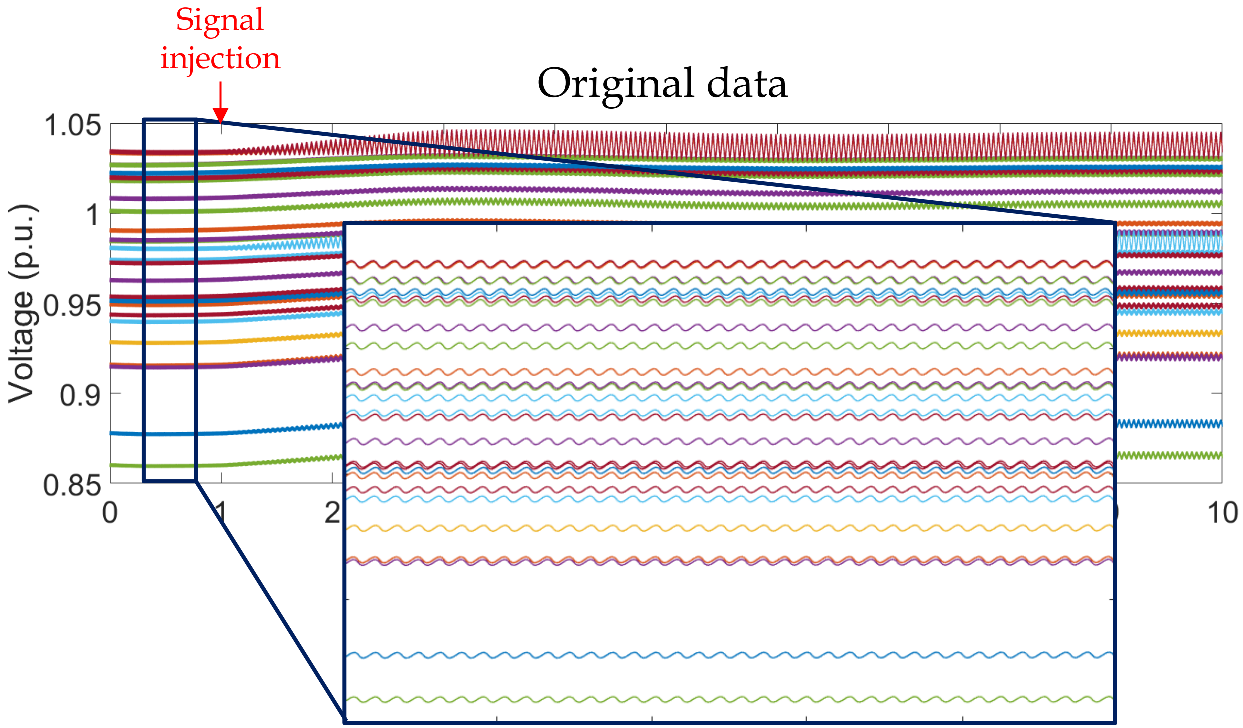

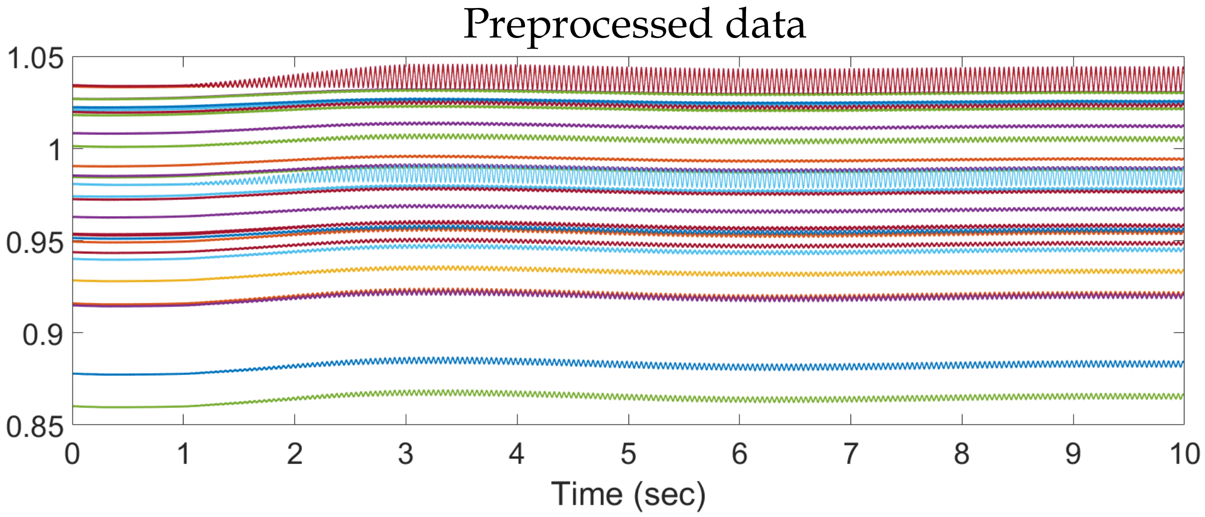

Experimental Results on SSO

- OSL Results for SSO Case 1 (Bus 38 Injection)
  - Oscillation detection
    - Detected at 1.0587s with 24.75 Hz estimated frequency
  - Source Location
    - Calculation starts at 1.2979s with computation time 1.9s
    - Largest OCF_{tt} values in lines 26_28 and 28_29 → Gen 38 as the oscillation source

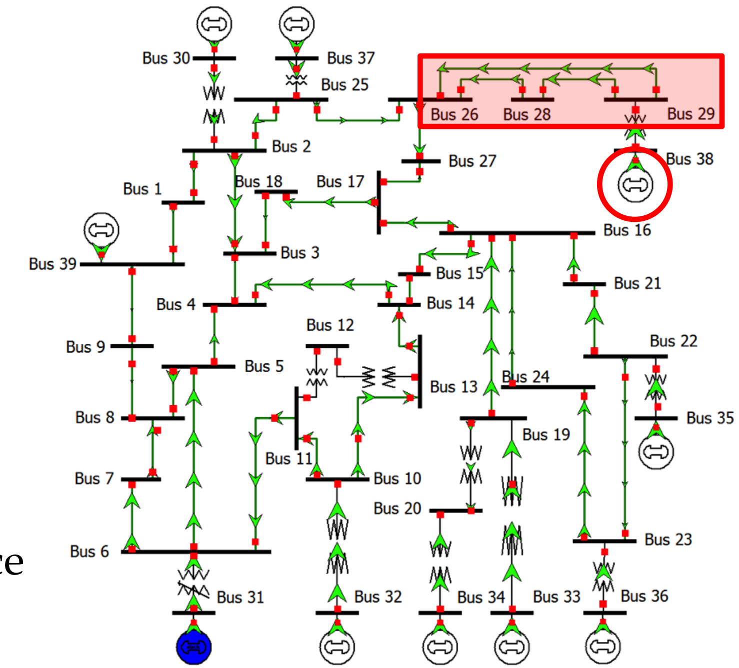

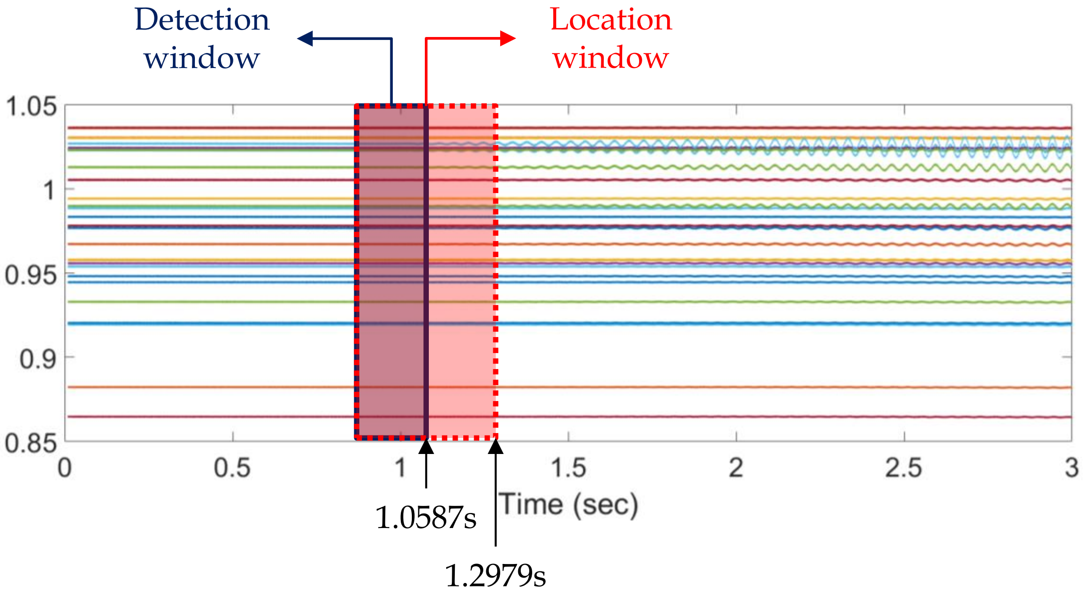

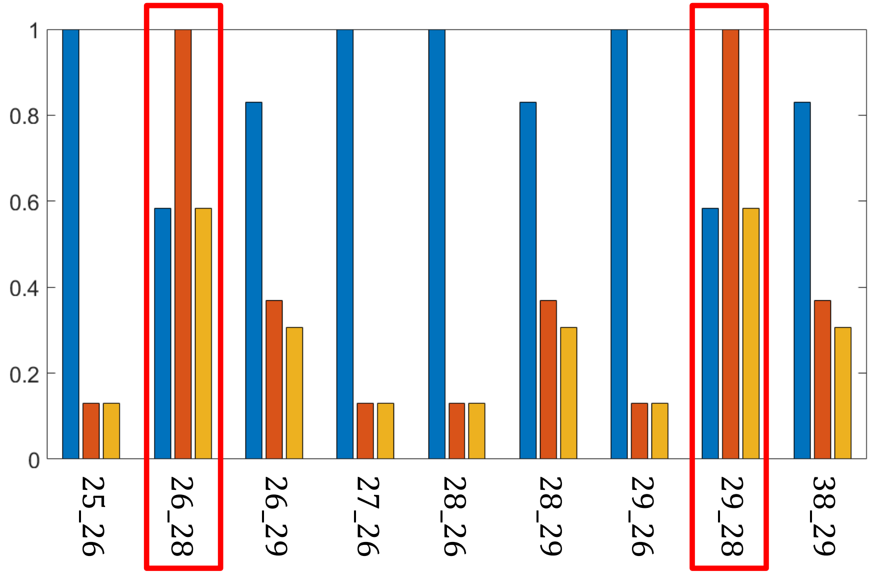

Experimental Results on SSO

- OSL Results for SSO Case 2 (Bus 39 Injection)
  - Oscillation detection
    - Detected at 1.0667s with 24.00 Hz estimated frequency
  - Source Location
    - Calculation starts at 1.3779s with computation time 3.3s
    - Largest OCF_{tt} values in lines 39_9 and 8_9 → Gen 39 as the oscillation source

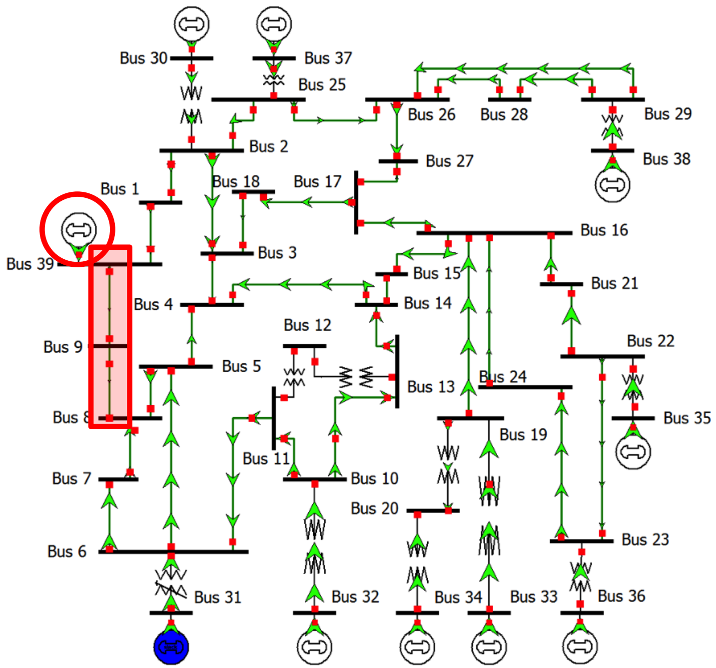

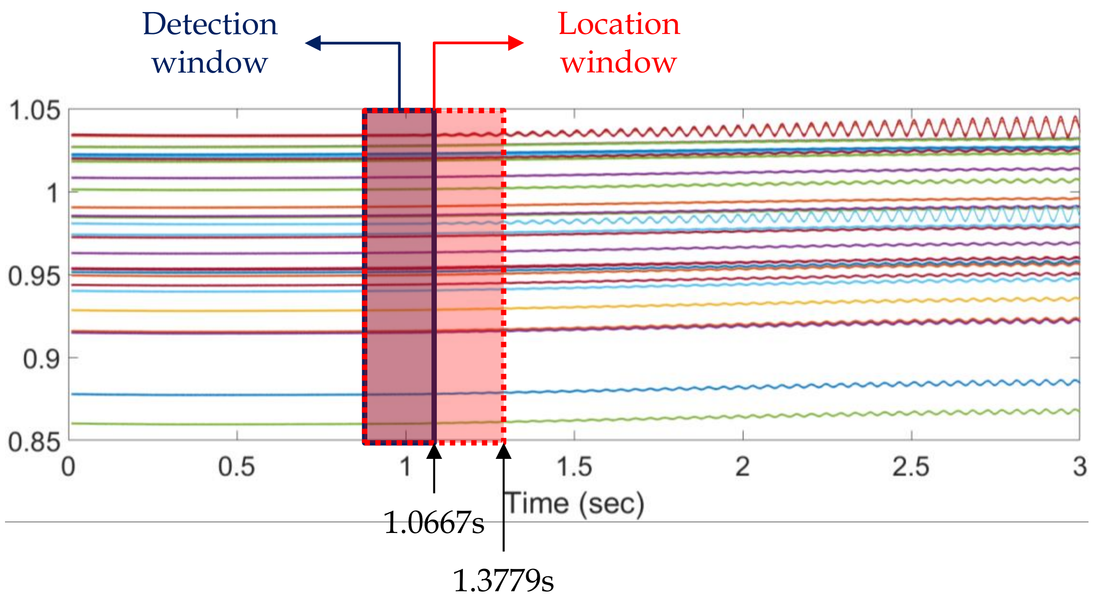

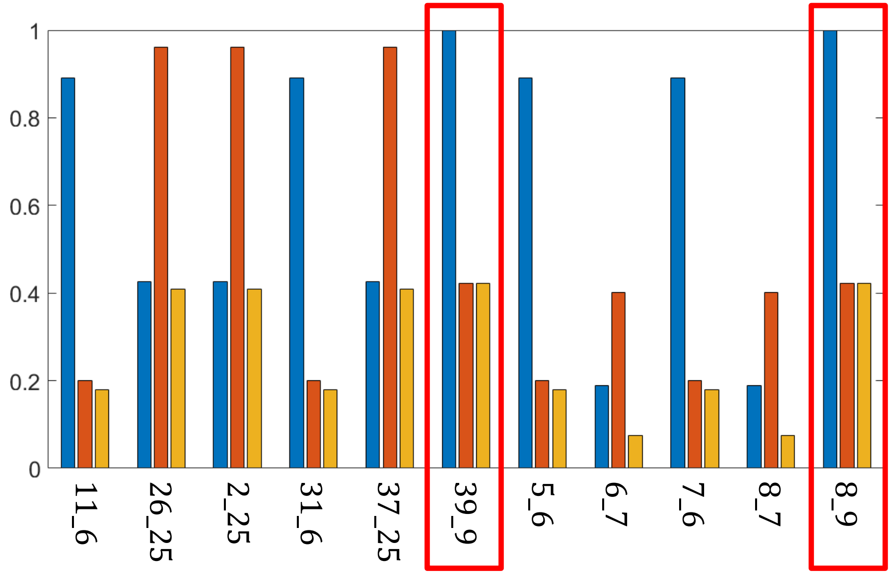

Conclusion

- OSL Framework with Improved DMD and Two-Tier Structure
  - **Improved DMD** including the initial state of the measurements as an additional input to enhance the clarity of the oscillation analysis
  - **Online oscillation detection** and followed oscillation **source location** framework
  - **Two-tier structure** with full-time and peak-time DMDs for enhancing accuracy of the source location on various oscillation categories
  - Validation of the proposed method on **forced & natural LFO** and **forced SSO** cases